Journal of ELECTRONIC MATERIALS, Vol. 39, No. 12, 2010
DOI: 10.1007/s11664-010-1382-2
© 2010 TMS

Reactions of Sn-3.5Ag-Based Solders Containing Zn and Al Additions on Cu and Ni(P) Substrates

H.R. KOTADIA,[1,3] O. MOKHTARI,[1] M. BOTTRILL,[2] M.P. CLODE,[1] M.A. GREEN,[2] and S.H. MANNAN[2]

1.—Department of Mechanical Engineering, King's College London, Strand, London WC2R 2LS, UK. 2.—Department of Physics, King's College London, Strand, London WC2R 2LS, UK. 3.—e-mail: hiren.kotadia@kcl.ac.uk

In this study we consider the effect of separately adding 0.5 wt.% to 1.5 wt.% Zn or 0.5 wt.% to 2 wt.% Al to the eutectic Sn-3.5Ag lead-free solder alloy to limit intermetallic compound (IMC) growth between a limited volume of solder and the contact metallization. The resultant solder joint microstructure after reflow and high-temperature storage at 150°C for up to 1000 h was investigated. Experimental results confirmed that the addition of 1.0 wt.% to 1.5 wt.% Zn leads to the formation of Cu-Zn on the Cu substrate, followed by massive spalling of the Cu-Zn IMC from the Cu substrate. Growth of the Cu_6Sn_5 IMC layer is significantly suppressed. The addition of 0.5 wt.% Zn does not result in the formation of a Cu-Zn layer. On Ni substrates, the Zn segregates to the Ni_3Sn_4 IMC layer and suppresses its growth. The addition of Al to Sn-3.5Ag solder results in the formation of Al-Cu IMC particles in the solder matrix when reflowed on the Cu substrate, while on Ni substrates Al-Ni IMCs spall into the solder matrix. The formation of a continuous barrier layer in the presence of Al and Zn, as reported when using solder baths, is not observed because of the limited solder volumes used, which are more typical of reflow soldering.

Key words: Pb-free solder, intermetallic, interfacial reactions, Sn-Ag solder alloy, spalling

INTRODUCTION

Implementation of Pb-free solder manufacturing has become increasingly important in recent years due to environmental concerns.[1,2] Therefore, the interfacial reaction between Pb-free solder (Sn-Ag, Sn-Cu, and Sn-Ag-Cu) and Cu or Ni(P) [electroless nickel-immersion gold (ENIG)] substrates during reflow and aging as well as their mechanical properties have attracted much attention over the past decade.[2–6] In these Sn-based alloys, Sn is the main active element and reacts with the Cu and Ni(P) substrates to form Cu-Sn and Ni-Sn intermetallic compound (IMC) layers. However, solder joints are not generally reliable at temperatures above 125°C.[7,8] This is due to the fact that, although formation of an IMC layer between the barrier metal and the molten solder is necessary to achieve an adhesive bond, excessive IMC formation may cause brittle failure. Traditionally trace amounts of certain elements, i.e., rare-earth elements, have proven to be effective in suppressing the growth of Cu-Sn IMC layers and consequently improved long-term reliability of the solder joint.[9] Recently, several researchers[9–15] have demonstrated that the addition of small quantities of Al or Zn can suppress Cu-Sn IMC layer growth.

Previous studies on Al additives to solders have concentrated on Al additives to solder baths. The role of Al addition to solder baths in suppressing Cu_6Sn_5 interfacial IMC growth on Cu substrates has been reported.[11] The present paper extends these previous studies by considering the effects of the additives to smaller solder volumes representative of reflow soldering rather than solder baths. The effects of Zn addition on properties such as drop,[10] tensile,[16,17] and creep resistance[18,19] have been

(Received May 26, 2010; accepted September 6, 2010; published online October 1, 2010)

reported in Sn-Zn and Sn-Cu-Zn reflow soldering systems. This report extends the study to Sn-Ag-Zn systems and specifically concentrates on the effects of long-term aging. The use of Al and Zn in solder paste and reflow soldering is generally avoided because of excessive oxidation of solder particles leading to poor wetting. The addition of these elements in such a manner as to avoid these problems is not explicitly addressed in this paper as it is the subject of ongoing research,[20] but the solder volumes studied in this work are more representative of reflow soldering. One consequence of the smaller solder volumes is the occurrence of massive spalling of Al- and Zn-containing IMCs from the substrate as the active element is depleted from the solder, changing the thermodynamically stable phase at the interface between the solder and the substrate.[21]

The present study is focused on the interfacial reaction between the Sn-3.5Ag solder alloy with varying levels of Zn and Al addition on two different substrates [Cu and Ni(P)] during reflow and high-temperature storage at 150°C for up to 1000 h. The addition of Al to the Sn-Ag basic solder resulted in Ag-Al particles forming in the solder matrix, and Al-Cu and Al-Ni IMC particles spalling into the solder matrix from the solder–substrate interface. The addition of up to 1.5 wt.% Zn to the Sn-Ag basic solder led to significant suppression of Cu_6Sn_5, Cu_3Sn, and Ni_3Sn_4 IMC growth. With the Zn concentration between 1 wt.% and 1.5 wt.% massive spalling of the Cu-Zn IMC from the Cu substrate was observed. We also note that Zn addition significantly changes the wettability of the Sn-Ag solder alloy on Cu and Ni(P) substrates.

EXPERIMENTAL PROCEDURES

Alloy Preparation

The eutectic Sn-3.5Ag solder alloy was supplied by Henkel Ltd., UK. Predetermined quantities of Sn-Ag ingots and Al foil were mechanically compressed and placed in a quartz tube sealed into an electric resistance furnace with vacuum (10^{-5} Torr), and those with Zn alloys were prepared in an electrical resistance furnace in air. The Sn-Ag solder alloys with 0.5 wt.% to 2 wt.% Al are referred to hereinafter as Sn-Ag-Al solder and those with Zn (0.5 wt.%, 1 wt.%, 1.5 wt.%) as Sn-Ag-0.5Zn, Sn-Ag-1Zn, and Sn-Ag-1.5Zn solder, respectively. All compositions herein are given in weight percent unless otherwise stated.

Preparation of Samples

Ni(P) substrates supplied by Schlumberger consisted of electroless Ni immersion gold (ENIG) bond pads on polyimide boards. The Cu substrates consisted of Cu-coated FR4. Both Ni(P) and Cu substrates were cut into ~5 mm square plates with metal thickness of ~40 μm. Before reflowing, the substrate was cleaned using isopropyl alcohol (IPA), acetone, and finally deionized water. For all the alloys, 0.012 ± 0.003 g solder alloy was cut from the ingot, coated by a thin layer of flux, and placed onto the substrate. The reflow was carried out in air: preheating at 140°C for 150 s and soldering at 260°C for 60 s. The resulting solder had a maximum thickness of 1 mm at the top of the solder dome, and the average solder thickness was 0.54 mm. High-temperature storage was carried out in air at 150°C for up to 1000 h. After reflow and storage, the samples were cross-sectioned and polished using SiC abrasive papers and 0.25-μm diamond suspension solution.

DSC Tests

Differential scanning calorimetry (DSC) tests were carried out using a Mettler Toledo DSC 822 differential scanning calorimeter. For all DSC tests, the heating (melting) and cooling (solidification) rate was fixed at 10°C min^{-1} from 25°C to 250°C, and the solder alloy mass was 0.025 ± 0.005 g. The thermal behaviors of the solders were recorded during heating and cooling in the calorimeter, and the cooling behaviors were compared with the results obtained from microstructural analysis. Each solder alloy test was repeated at least twice to ensure reproducibility of results.

Microscopy

The microstructures were observed without etching under a ZEISS Axioscop2 MAT optical microscope equipped with an automated Zeiss AxioVision image analyzer, which was used for the microstructural investigation and quantitative morphology analysis. An FEI scanning electron microscope (SEM) equipped with energy-dispersive spectroscopy (EDX) at an accelerating voltage of 25 kV was used to achieve higher magnification in areas of interest, as well as to quantitatively identify each phase region. To quantify the uniformity of the IMC layer thicknesses, the IMC thickness data for all solder alloys on Cu and Ni(P) substrate samples were measured using image analysis software.

RESULTS AND DISCUSSION

Effect of Solder Alloy Composition on Melting and Solidification

The amount of undercooling and the melting point measured for Sn-3.5Ag solder alloys with different Zn and Al contents were measured by DSC and are listed in Table I. DSC plots are presented in Fig. 1. Heating and cooling rates of 10°C min^{-1} were used. As the concentration of Zn was increased, both the melting temperature and the amount of undercooling dropped. Increasing the concentration of Al, however, increased the melting temperature while still reducing undercooling. The undercooling (ΔT) was determined as the temperature difference between the melting point on the heating curve and

Table I. Differential scanning calorimetry (DSC) test results for solder alloys

Alloy Composition (wt.%)	Onset Melting Temperature During Heating (T_1, °C)	Onset Solidification Temperature During Cooling (T_2, °C)	Undercooling, $\Delta T = T_1 - T_2$ (°C)
Sn-3.5Ag	219.15	204.24	14.91
(Sn-3.5Ag)-0.5Zn	220.25	216.86	3.39
(Sn-3.5Ag)-1Zn	217.19	215	2.19
(Sn-3.5Ag)-1.5Zn	216.3	214.89	1.41
(Sn-3.5Ag)-0.5Al	221.15	213.99	7.35
(Sn-3.5Ag)-1Al	221.72	215.31	6.41
(Sn-3.5Ag)-2Al	225.96	219.93	6.03

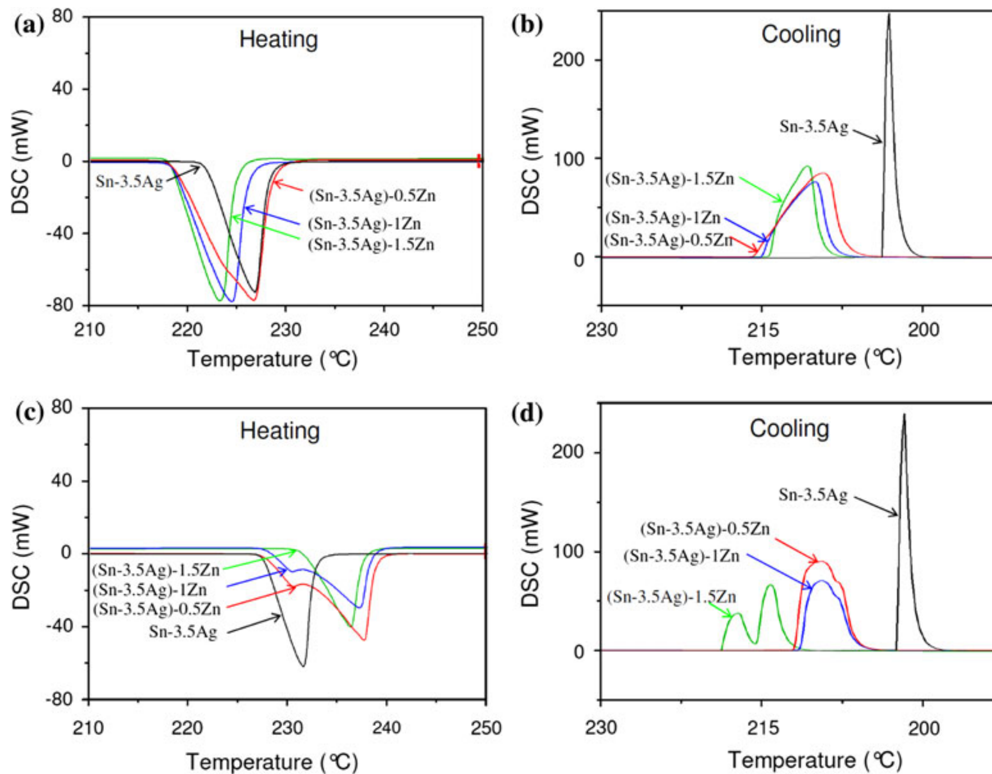

Fig. 1. DSC thermal profiles recorded during heating and cooling cycles of solder alloys: (a) and (b) with the addition of Zn to eutectic Sn-3.5Ag solder alloy; (c) and (d) with the addition of Al to eutectic Sn-3.5Ag solder alloy, during heating and cooling at 10°C min^{-1}.

the onset temperature of solidification on the cooling curve. The fact that undercooling was significantly reduced by the addition of small amounts of Zn and Al suggests that the original Ag_3Sn IMC present in pure Sn-3.5Ag solder does not provide preferential nucleation sites during β-Sn solidification. For (Sn-3.5Ag)-Al solder alloys, additional small peaks are observed in Fig. 1c, d. These could indicate the formation of Ag-Al phases, which were observed in microscopic analysis.

Liquid- and Solid-State Reactions in the Sn-Ag-Zn/Cu System

Figure 2 shows typical cross-sectional SEM images of the Sn-Ag/Cu and Sn-Ag-Zn/Cu systems after reflow and during subsequent aging. The interfacial reaction between Sn-Ag and the Cu substrate initially forms a scallop-shaped η-Cu_6Sn_5 layer (Fig. 2a). After a few hours of subsequent aging, an ε-Cu_3Sn IMC layer developed between the η-Cu_6Sn_5 and the Cu. This has been widely observed previously in Sn-based solder alloy systems.[7]

Electron microprobe analysis and energy-dispersive x-ray spectroscopy (EDX) were used to detect possible segregation of Zn atoms during interfacial reactions of solder on Cu substrates. The IMCs formed on the interface and solder matrix strongly depended on the amount of Zn addition to the basic Sn-Ag solder alloy. On Cu substrates, immediately after reflow (260°C for 60 s), 0.5 wt.% Zn addition made only slight differences to IMC

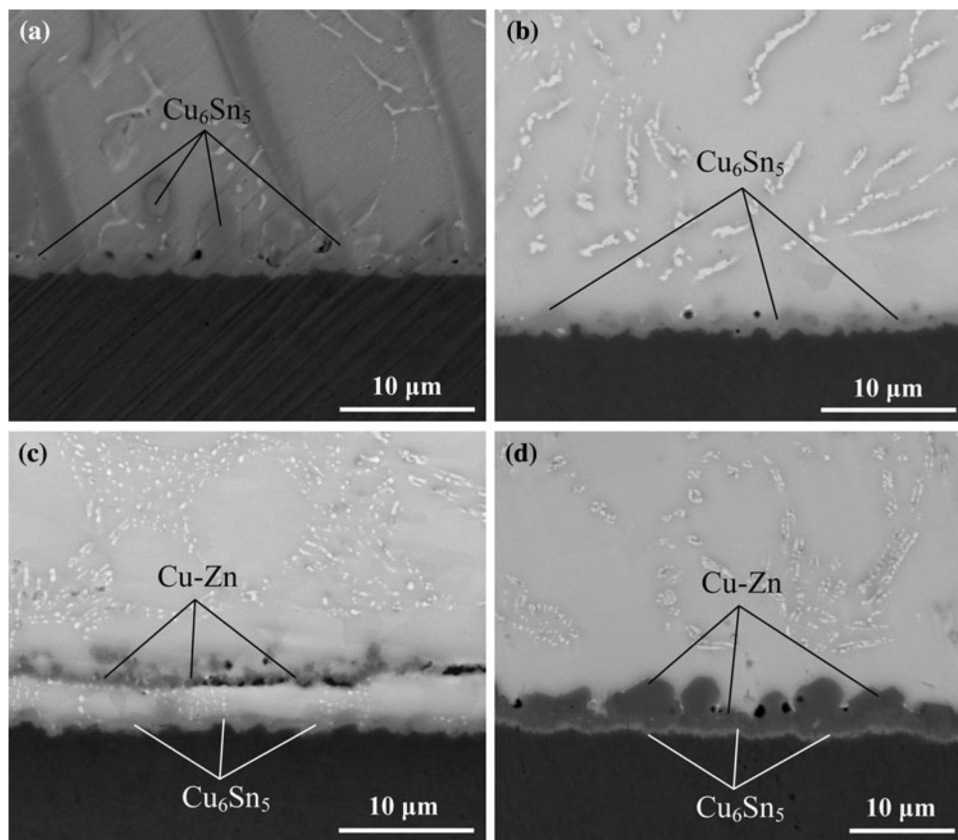

Fig. 2. SEM images showing interfacial reactions between solder/Cu: (a) Sn-3.5Ag, (b) (Sn-3.5Ag)-0.5Zn, (c) (Sn-3.5Ag)-1Zn, and (d) (Sn-3.5Ag)-1.5Zn solder alloys, after reflow.

cross-section microstructure, and Cu_6Sn_5 IMC formed at the solder/Cu interface (Fig. 2b). By contrast, the addition of 1 wt.% to 1.5 wt.% Zn resulted in Cu-Zn IMC formation, followed by massive spalling at the interface (Fig. 2c, d), just after reflow. The composition of the Cu-Zn layer was determined by EDX to be 13 at.% Sn, 45 at.%. Cu, and 42 at.% Zn. In total, two IMC layers were identified at the interface: a Cu_6Sn_5 IMC adjacent to the Cu substrate, and a Cu-Zn-based compound in the solder itself, while the gap between the Cu-Zn and Cu_6Sn_5 layers was occupied by solder. The average thickness of the Cu-Zn spalled layer was measured to be 2 μm to 4 μm. This type of spalling has been observed previously between a Sn-Zn solder and a Cu substrate.[21] Such massive spalling was attributed to the possibility that the original reaction product at the interface is no longer in local thermodynamic equilibrium with the solder, and this compound is driven away to make room for the nucleation and growth of the equilibrium phase. Initially Cu-Zn IMCs nucleate and grow at the interface, but after consumption of Zn atoms from the limited solder volume, Cu_6Sn_5 becomes the thermodynamically favored phase and the Cu-Zn spalls away from the substrate. Figure 3 delineates the elemental distribution after reflow at 260°C for 60 s. It is seen that Zn segregates at the Sn-Ag-(1-1.5)Zn/Cu system interfaces. The analysis line passes through the interfacial IMC layer and shows an overlap of Cu and Zn in the Sn-Ag-(1-1.5)Zn/Cu system, indicating Cu-Zn IMC formation. It is thus clear that the addition of 1 wt.% and 1.5 wt.% Zn causes the formation of an IMC, while at 0.5 wt.% no Cu-Zn IMC layer or particles form. This is consistent with the work of Chou and Chen,[22] who reported a thermodynamic study showing that higher Zn concentration levels result in Cu_5Zn_8 being the more thermodynamically stable phase on Cu substrate. The addition of Zn to Sn-Ag solder alloys also reduced Ag_3Sn plate size as expected from the DSC undercooling results and similar results from the Sn-3.8Ag-0.7Cu solder alloy.[13]

During the process of thermal aging, IMCs grow continuously due to element diffusion, resulting in morphology changes and thickness increase. The average IMC thickness and the morphology at the interface were studied during isothermal aging at 150°C, for up to 1000 h, as shown in Fig. 4. For the Sn-Ag/Cu system (Fig. 4a), we saw a monotonic increase in IMC layer thickness as a function of storage time. In the Sn-Ag-Zn/Cu systems, the presence of Zn significantly suppressed Cu_6Sn_5 IMC growth even after prolonged storage time

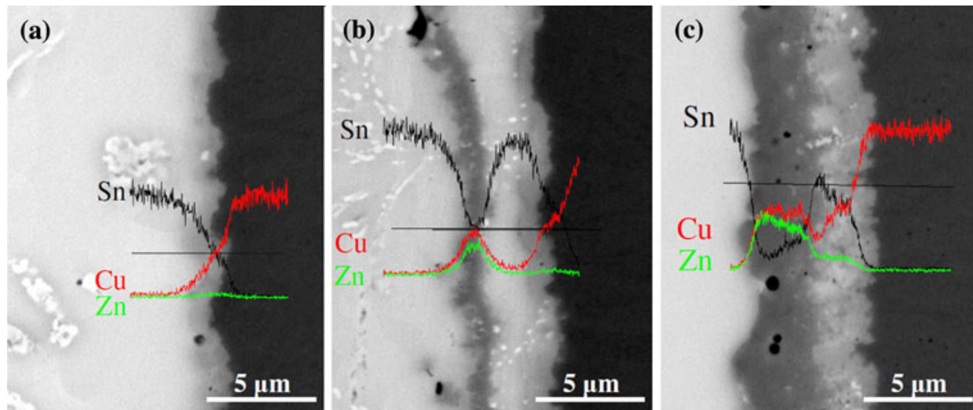

Fig. 3. Elemental analysis of (a) (Sn-3.5Ag)-0.5Zn, (b) (Sn-3.5Ag)-1Zn, and (c) (Sn-3.5Ag)-1.5Zn solder alloys on Cu substrates, after reflow.

(although the effect was less pronounced for the Sn-Ag-0.5Zn/Cu system). During the aging process, continuous growth of the Cu_6Sn_5 phase and spalling of individual Cu_6Sn_5 particles from the IMC layer were observed. This type of spalling occurs by transformation from a hemispherical to a more spherical type of particle, driven by lowering of the total surface and interfacial energies in conservative ripening.[4,5,23–25] After 1000 h of storage the Sn-Ag-0.5Zn/Cu system showed significant spalling at the interface, marked by arrows in Fig. 4a. In contrast to the Sn-Ag/Cu and Sn-Ag-0.5/Cu systems, the Sn-Ag-1Zn/Cu and Sn-Ag-1.5/Zn systems showed significant suppression of Cu_6Sn_5 IMC layer growth (limited to 3 μm after 1000 h of storage time at 150°C). It was found that the Cu-Zn IMC layer thickness does not change as a function of storage time and remained at between 2 μm and 4 μm up to 1000 h at 150°C (Fig. 4c).

Another observation was that, at the Sn-Ag-(0.5-1.5)Zn/Cu system interface, the Cu_3Sn IMC layer only grew to about 1 μm after 1000 h of high-temperature storage (Fig. 4b). The initiation of Cu_3Sn phase formation in the Sn-Ag/Cu system generally occurs after a few hours of storage time, but the presence of Zn appears to have delayed formation of the Cu_3Sn phase. The suppression of the Cu_3Sn would then be expected to improve mechanical and electromigration reliability.[14]

Figure 5 shows cross-sectional views of Sn-Ag/Cu and Sn-Ag-Zn/Cu samples after 1000 h of storage time. In the Sn-Ag/Cu system, cracks at the substrate/IMC interface were observed after high-temperature storage for 360 h (see Fig. 5a for a typical crack image). By contrast, these cracks did not occur in the Sn-Ag-Zn/Cu systems. A previous study by Yao and Shang[26] reported that fatigue crack growth is suppressed with improvements in interfacial IMC smoothness, further suggesting that Zn-containing alloys are promising candidates from a reliability point of view. The layer of solder between the Cu-Zn IMC and Cu_6Sn_5 IMC visible in Fig. 2c, d, showing the same system immediately after reflow, has now been almost entirely consumed by further growth of the Cu_6Sn_5 layer (Fig. 5c, d). Small isolated pockets of solder remain at the interface between the two IMC layers, but the interface is otherwise almost completely planar, and the Cu-Zn IMC therefore acts as a barrier layer to further Cu_6Sn_5 layer growth. In particular, the Cu-Zn must act as a barrier layer to further diffusion of Sn in order to limit the thickness of the Cu_6Sn_5 layer, and the absence of Cu_6Sn_5 particles in the solder matrix shows that the Cu-Zn layer also blocks Cu diffusion.

After aging, the Cu_6Sn_5 and Cu_3Sn IMC thickness decreases as the Zn concentration increases. To identify the phenomena responsible, further composition analysis was carried out on the (Sn-3.5Ag)-1Zn/Cu system after 1000 h of storage. The interfacial cross-section after 1000 h is shown in Fig. 6. The line scan at the interface shows the elemental distributions of Sn, Cu, and Zn. Segregation of Zn at the Cu_6Sn_5/Cu substrate interface is indicated by the arrow in Fig. 6. Several line scans at multiple locations all confirmed the segregation of Zn at this interface after long-term storage. This accumulation of Zn could form a thin Cu-Zn IMC layer at the interface and retard further Cu and Sn diffusion at the substrate.[19,27] While the much thicker Cu-Zn barrier layer at the Cu_6Sn_5/solder interface blocks diffusion of Sn and limits further Cu_6Sn_5 growth, the thin Cu-Zn barrier at the substrate interface helps to retard Cu_3Sn IMC formation. Table II summarizes the different types of IMCs observed on Cu substrates.

The growth kinetics of Sn-based alloys on Cu substrates, below the melting point of Sn, generally follows a parabolic law as a result of diffusion of Sn through the Cu_6Sn_5 layer:

$$d = k(t)^{1/2} + d_0, \tag{1}$$

where d and d_0 are the thickness of the IMC at time t and zero, respectively, and k is the growth rate constant.[28] The growth rate constant (k) was calculated from a linear regression analysis of IMC

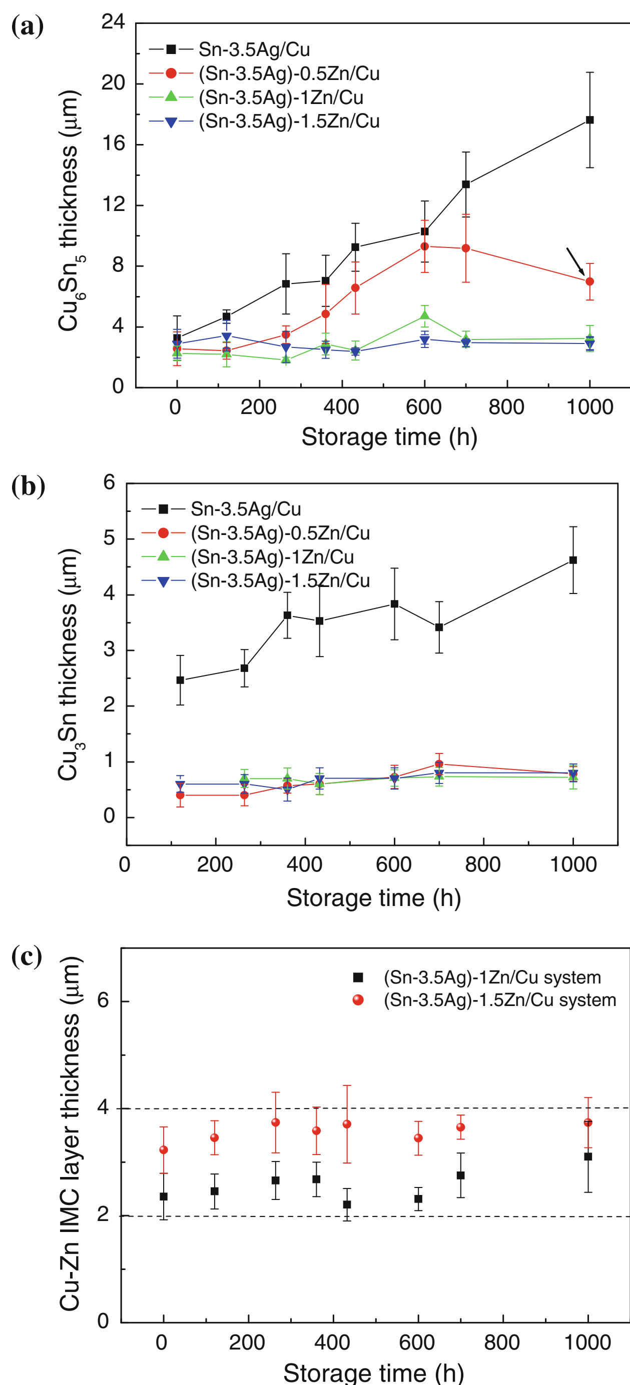

Fig. 4. Intermetallic compound (IMC) thickness as a function of aging time: (a) Cu_6Sn_5/Cu, (b) Cu_3Sn/Cu, and (c) Cu-Zn/Cu interfaces. Note that the reflow condition for all the samples was 260°C for 60 s, and the storage temperature was 150°C.

thickness $d - d_0$ versus $t^{1/2}$, where the slope is k. According to the data in Fig. 4a, b, the k^2 values of Cu_6Sn_5 and Cu_3Sn layer growth in Sn-Ag-(0.5-1.5)Zn/Cu systems are much lower than in the Sn-Ag/Cu system (Table III). The exact mechanism of growth suppression is not understood, but from Fig. 3 it is clear that Zn is present in small quantities in the Cu_6Sn_5 layer and may be affecting Sn diffusion, while the activity of Sn will also be affected by even trace amounts of Zn.[9]

A solder should have good wetting properties. The average wetting angle at 260°C in the Sn-Ag-Zn/Cu system was measured by using a Zeiss AxioVision image analyzer, using the eutectic Sn-3.5Ag solder as a baseline, and is tabulated in Table IV. The Sn-Ag/Cu system average wetting angle was measured to be 28.5°, while a monotonic rise of wetting angle with increasing concentration of Zn was observed. Research is currently underway into introducing Zn (and Al) into the solder paste in the form of Ag-capped nanoparticles that release the Zn or Al loads after solder wetting has occurred. Previous work on chemically passive, coated nanoparticles suggests that this approach is likely to succeed.[29]

Liquid- and Solid-State Reactions in the Sn-Ag-Zn/Ni(P) Systems

A large volume of literature has been published on the interaction between Ni(P) and Sn-based solder alloys.[2–6] Figure 7a shows an SEM micrograph of the Sn-Ag/Ni(P) interface. Ni_3Sn_4, NiPSn, and Ni_3P layers form between the solder and Ni(P) substrate, as expected.[25] The Ni_3Sn_4 IMC growth can also be described by Eq. 1 with new parameters, which are determined experimentally.

In contrast to the Sn-Ag-Zn/Cu system, the Sn-Ag-Zn/Ni(P) system interface does not show formation and massive spalling of a Ni-Zn IMC (Fig. 7). The surface of the Ni_3Sn_4 layer in Sn-Ag-Zn/Ni(P) systems is also of the scallop type, but compared with the Sn-Ag/Ni(P) system, exhibits a smoother interface between solder and Ni_3Sn_4. Strictly speaking, this compound should be referred to as $(Ni_{1-x},Zn_x)_3Sn_4$, as the composition measured by EDX was 50 at.% Sn, 34 at.% Ni, and 16 at.% Zn, but for brevity we will refer to it as Ni_3Sn_4. Figure 8 delineates the elemental distribution in Sn-Ag-(0.5-1.5)Zn/Ni(P) systems, after reflow at 260°C for 60 s. This reveals that Zn segregation is undetectable at the interface when the Zn concentration in the solder is 0.5 wt.%, but very clear as the Zn concentration is increased to 1 wt.% and 1.5 wt.%. In addition, the thickness of the Ni_3Sn_4 IMC layer decreased with increasing Zn concentration.

During aging at 150°C the high-aspect-ratio Ni_3Sn_4 grains transformed to a much rounder shape (compare Fig. 7 with 10). In addition, some isolated Ni_3Sn_4 particles were found to have departed from the main Ni_3Sn_4 IMC layer and entered the solder matrix, contributing to a large degree of scatter and deviation from the expected parabolic growth. The Ni_3Sn_4 IMC layers formed in the Sn-Ag-Zn/Ni(P) systems were thinner than those in the Sn-Ag/Ni(P) system, for the same storage time, as shown in Fig. 9. Between 700 h and 1000 h, significant spalling of Ni_3Sn_4 particles was observed in all systems (Fig. 10), reducing interfacial IMC thickness.

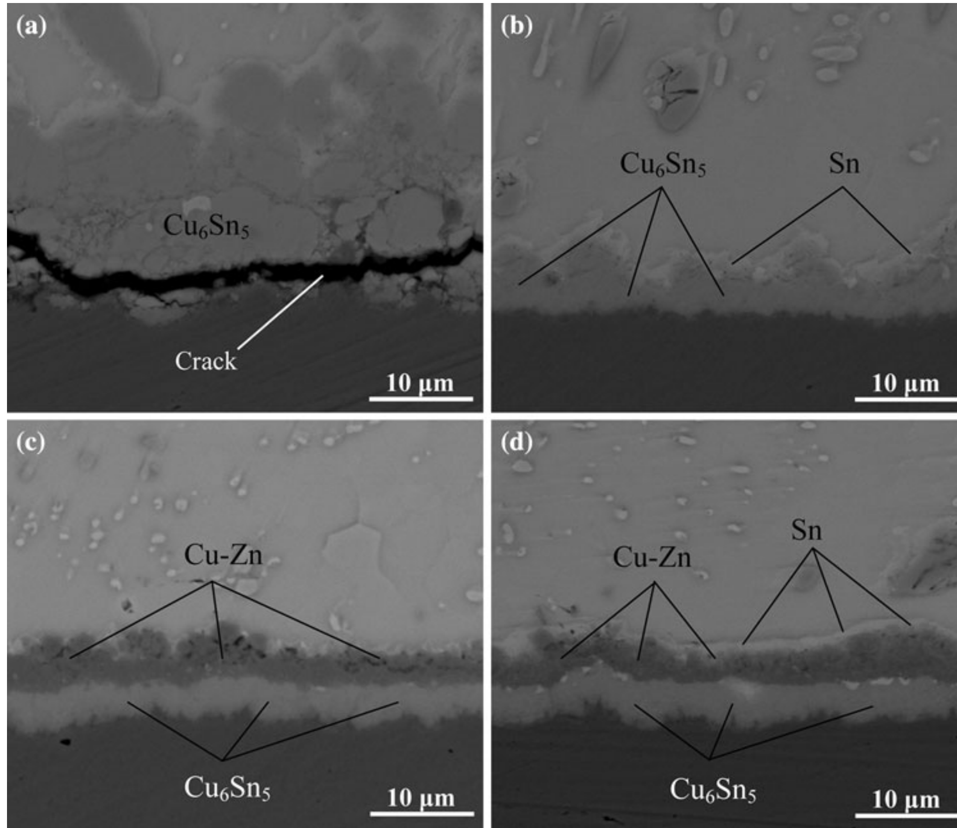

Fig. 5. SEM images showing interfacial reactions between solder/Cu: (a) Sn-3.5Ag, (b) (Sn-3.5Ag)-0.5Zn, (c) (Sn-3.5Ag)-1Zn, and (d) (Sn-3.5Ag)-1.5Zn solder alloys, after 1000 h of storage time at 150°C.

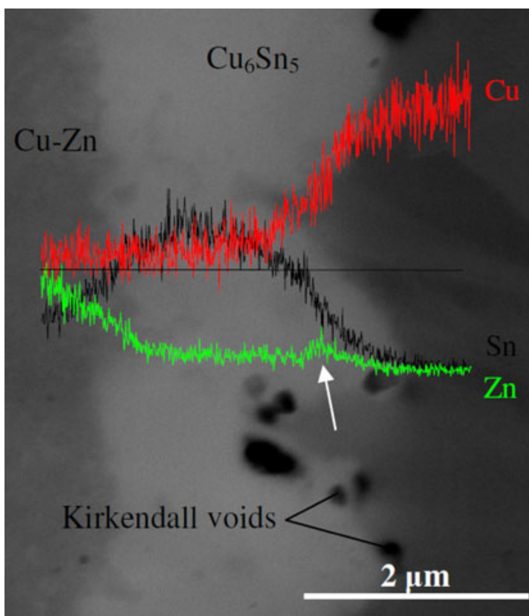

Fig. 6. Higher-magnification SEM image of the interface in the (Sn-3.5Ag)-1Zn/Cu system after aging for 1000 h at 150°C. The *arrow* shows Zn accumulation at the Cu substrate.

The IMC growth rates in the Sn-Ag/Ni(P) system are much larger than those in the Sn-Ag-Zn/Ni(P) systems, as shown by the growth rate constant (k) coefficients listed in Table III. Note also that the presence of Zn in the solder had a comparatively weaker effect on wetting angle for the Ni(P) substrate. The average wetting angles of Sn-Ag/Ni(P) and Sn-Ag-Zn/Ni(P) systems are presented in Table IV, and the different IMC layers and particles formed on Ni(P) substrates are presented in Table II.

Wang et al.[30] note that Zn addition to the Sn-based solder significantly reduced diffusion coefficients and may also decrease the activity of Sn atoms, which explains suppression of the IMC layer growth. Feng et al.[31] have studied the ternary Sn-Cu-Zn alloy, suggesting that the presence of Zn atoms seriously weakens the interaction between the Sn and Cu atoms, which decreases the diffusion and activity of Sn atoms. In summary, Table III shows that Sn-3.5Ag solder has large values for growth rate constants on both Cu and Ni(P) substrates, which significantly decrease with increasing Zn concentration in the solder. Increasing Zn concentration does, however, also raise wetting angles on both substrates.

Liquid- and Solid-State Reactions in the Sn-Ag-Al/Cu and Sn-Ag-Al/Ni(P) Systems

It is well known that Al has high chemical activity in molten solder, and will react with the substrate

Table II. Observed interfacial IMC layers and particles on solder samples after reflow on Cu and Ni(P) substrates

Alloy Composition (wt.%)	Cu Substrate	Ni(P) Substrate
Sn-3.5Ag	Cu_6Sn_5, Cu_3Sn IMC layer	Ni_3Sn_4, NiPSn, Ni_3P IMC layer
(Sn-3.5Ag)-0.5Zn	Cu_6Sn_5, Cu_3Sn IMC layer	Ni_3Sn_4, NiPSn, Ni_3P IMC layer
(Sn-3.5Ag)-1Zn	Cu_6Sn_5, Cu_3Sn, Cu-Zn IMC layer	Ni_3Sn_4, NiPSn, Ni_3P IMC layer
(Sn-3.5Ag)-1.5Zn	Cu_6Sn_5, Cu_3Sn, Cu-Zn IMC layer, and Cu_5Zn_8 particles	Ni_3Sn_4, NiPSn, Ni_3P IMC layer

Note that Sn-Ag and Sn-Ag-Zn solder alloys after reflow consisted of primary Sn-rich dendrite (β-Sn) phase surrounded by a eutectic mixture of Sn and Ag_3Sn plates.

Table III. Results of k (growth rate constant) value measurements for Cu_6Sn_5, Cu_3Sn, and Ni_3Sn_4 IMCs on Cu and Ni(P) substrates with different solder alloys

Alloy Composition (wt.%)	k^2 (m^2 s^{-1} × 10^{-19})[a]		
	Cu_6Sn_5	Cu_3Sn	Ni_3Sn_4
Sn-3.5Ag	535	24	136.9
(Sn-3.5Ag)-0.5Zn	144	1.8	17.6
(Sn-3.5Ag)-1Zn	14.4	0.47	19.8
(Sn-3.5Ag)-1.5Zn	7.9	0.44	5.8

[a]The growth rate constant (k) was calculated from linear regression analysis of IMC thickness $d - d_0$ versus $t^{1/2}$, where the slope is k.

Table IV. Contact angles of eutectic Sn-3.5Ag and (Sn-3.5Ag)-(0.5-1.5)Zn solder alloys on Cu and Ni(P) substrates

Alloy Composition (wt.%)	Avg. Contact Angle	
	Cu Substrate	Ni(P) Substrate
Sn-3.5Ag	28.5°	19.2°
(Sn-3.5Ag)-0.5Zn	36.7°	29.5°
(Sn-3.5Ag)-1Zn	48.8°	30.4°
(Sn-3.5Ag)-1.5Zn	58.0°	32.5°

Note that average contact angle is quantified from seven identical samples from each substrate.

materials present. At low concentrations of added Al, the Al formed distinct Ag_3Al IMC particles in the solder matrix during the solder alloy preparation. In the Sn-Ag-Al/Cu systems, Al reacts with Cu dissolving from the substrate to form Al_2Cu and other (not unambiguously identifiable) Al-Cu IMC phases in the solder matrix, as listed in Table V. In a study by Jee et al.,[11,12] the Al-Cu IMC appeared at the solder/substrate interface rather than in the solder. In the present study, due to the limited solder volume, Al was quickly depleted while forming the Al-Cu IMC, and Cu_6Sn_5 forms at the solder/substrate interface. Any Al-Cu that formed at the interface spalled off when the Al was depleted in the solder, and Cu_6Sn_5 becomes the thermodynamically stable phase, analogous to the Sn-Ag-Zn/Cu system, although in this case a continuous spalled layer was not visible (Fig. 11). Previous work[11,12] reported a thermodynamically stable Al-Cu IMC phase at the interface in the Sn-Ag-1.5Al/Cu system, and the difference was again attributable to the use of a solder bath in that study, maintaining the Al concentration in the solder.[21] Figure 11a–c are typical of the Sn-Ag-Al/Cu system irrespective of the exact Al concentration used up to 2 wt.%.

Analysis of the location of the Al-Cu IMC particles in Fig. 11 indicates that, during solidification, large Al-Cu particles that are present in the molten solder are pushed ahead by Sn-rich dendrites, which grow upwards from the substrate during solidification. Entrapment of smaller particles then occurs in the interdendritic region. These small particles form when Cu is extracted from the Sn-rich dendrites.

Similar experiments were carried out on Ni(P) substrates, and Al was found in the form of Al_3Ni_2 and Al-Ag IMC particles in the solder matrix immediately after reflow (Fig. 12). The Al_3Ni_2 IMC layer forms about ~5 μm from the Ni(P) substrate (Fig. 12), and although the layer is not continuous, the linear arrangement of the particles suggests that they spalled off the substrate.

In general, the volume percentage of the new IMC phase in the solder depends on the Al concentration and soldering time. Higher concentrations of Al significantly increase the rapid initial consumption of the substrate as the Al-containing IMCs are produced. Wetting of the solder was rendered particularly difficult by the presence of Al, and the solder had to be mechanically polished to remove oxidized Al prior to soldering. Storage at 150°C showed no suppression of interfacial IMCs on either Cu or Ni(P) substrates due to the absence of a stable Al-based IMC barrier layer at the substrate.

The observed differences between the Sn-Ag-Zn system and Sn-Ag-Al system in terms of IMC suppression and spalling of IMCs on both Cu and Ni(P) substrates is summarized in Table IV.

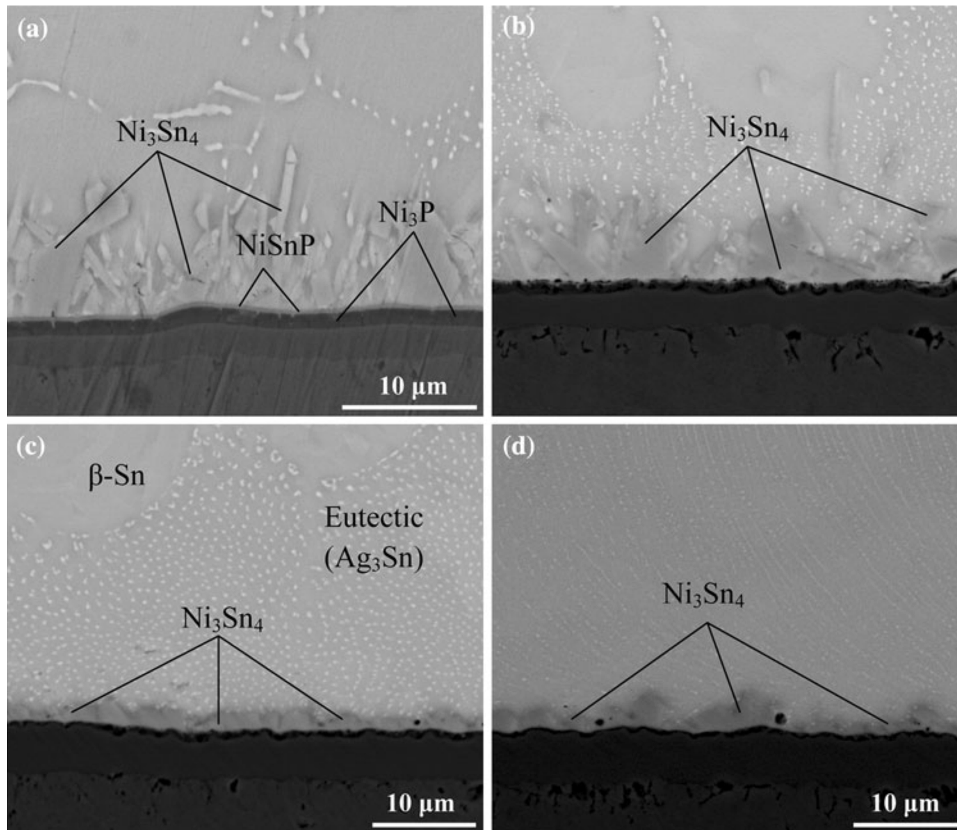

Fig. 7. SEM images showing interfacial reactions between solder/Ni(P): (a) Sn-3.5Ag, (b) (Sn-3.5Ag)-0.5Zn, (c) (Sn-3.5Ag)-1Zn, and (d) (Sn-3.5Ag)-1.5Zn solder alloys, after reflow.

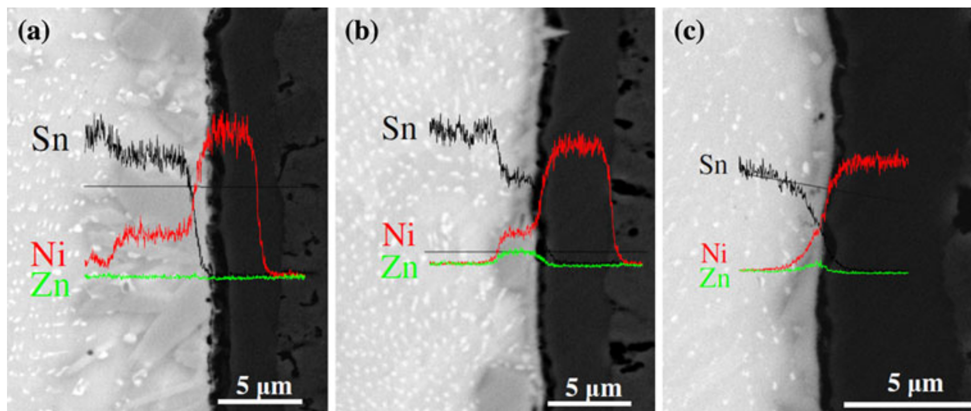

Fig. 8. Elemental analysis of: (a) (Sn-3.5Ag)-0.5Zn, (b) (Sn-3.5Ag)-1Zn, and (c) (Sn-3.5Ag)-1.5Zn solder alloys on Ni(P) substrates, after reflow.

CONCLUSIONS

Based on the experimental results and the above analysis, the following conclusions can be drawn.

DSC examination of the samples revealed signals corresponding to phase transitions during heating and cooling. Minor alloying elements Zn and Al reduced undercooling in Sn-3.5Ag solders with a slight decrease (addition of Zn) or a slight increase (addition of Al) in melting point.

It was found that 0.5 wt.% Zn addition did not result in considerable suppression of Cu_6Sn_5 IMC growth when Sn-Ag-0.5Zn/Cu samples were stored at 150°C for 1000 h. However, the IMC growth was significantly suppressed by 1 wt.% and 1.5 wt.% Zn addition to Sn-Ag solder. The formation of the Cu_3Sn IMC layer was also suppressed significantly

with Zn addition. Accumulation of Zn was found at the Cu substrate/Cu_3Sn interface.

Increasing the concentration of Zn to 1 wt.% and 1.5 wt.% results in massive spalling of the Cu-Zn IMC layer. This is interpreted as follows: The first reaction product at the interface is Cu-Zn IMC, which is not thermodynamically stable as the interface IMC after consumption of Zn atoms from the solder matrix. This allows the nucleation of the more thermodynamically stable phase (Cu_6Sn_5) in later stages of interface growth. During aging, the Cu_6Sn_5 layer grows until it reaches the Cu-Zn layer.

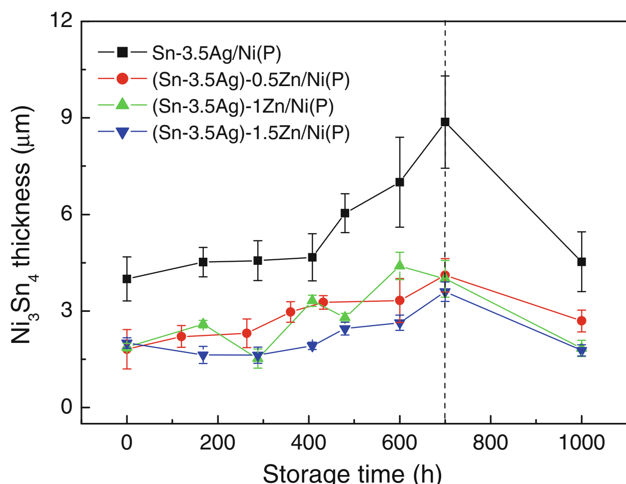

Fig. 9. Intermetallic compound (IMC) thickness as a function of aging time for Ni_3Sn_4/Ni(P); *dotted line* represents the onset of significant spalling. Note that the reflow condition for all the samples was 260°C for 60 s, and the storage temperature was 150°C.

In the Sn-Ag-Zn/Ni(P) system, a massive spalling effect is not seen and at the interface Ni_3Sn_4 $[(Ni_{1-x},Zn_x)_3Sn_4]$ IMC formed in all samples. Zn is found to be segregated in this IMC layer for Sn-Ag-1Zn and Sn-Ag-1.5Zn. However, after high-temperature storage for between 700 h and 1000 h, a significant amount of Ni_3Sn_4 IMC spalled from the interface and traveled into the solder matrix. The addition of Zn suppressed Ni_3Sn_4 IMC growth during solid-state isothermal aging. On both Cu and Ni(P) substrates, the IMC growth suppression effect increased with increasing concentration of Zn in the Sn-Ag solder. The contact angles similarly increased with increasing Zn addition to the solder.

The addition of Al to Sn-Ag solder alloys does not change the IMCs formed at the Cu and Ni(P) substrate interfaces. Al from the solder reacts with Cu from the substrate to form Al-Cu intermetallics, which spall away from the substrate during reflow, and the normal interfacial IMCs of Cu_6Sn_5 and Cu_3Sn are observed. In the case of the Ni(P) substrate,

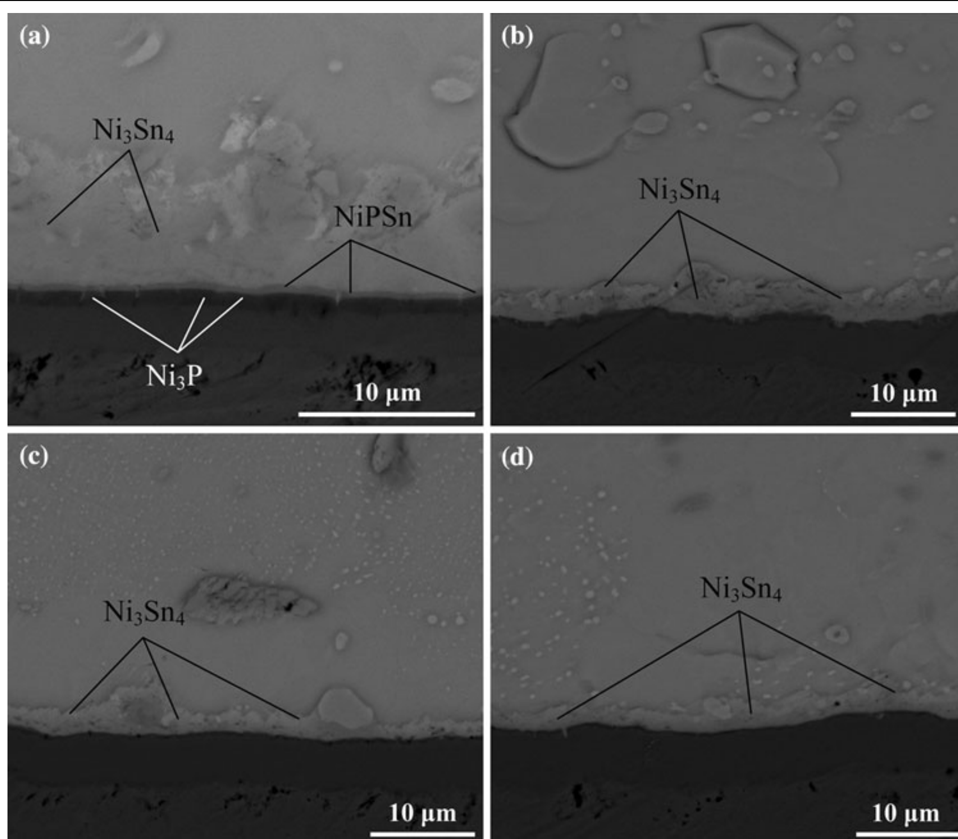

Fig. 10. SEM images showing interfacial reactions between solder/Ni(P): (a) Sn-3.5Ag, (b) (Sn-3.5Ag)-0.5Zn, (c) (Sn-3.5Ag)-1Zn, and (d) (Sn-3.5Ag)-1.5Zn solder alloys, after 1000 h of storage time at 150°C.

Table V. Observed interfacial IMC layers and particles on solder samples after reflow on Cu and Ni(P) substrates

Alloy Composition (wt.%)	Cu Substrate	Ni(P) Substrate
Sn-3.5Ag	Cu_6Sn_5, Cu_3Sn IMC layer	Ni_3Sn_4, NiPSn, Ni_3P IMC layer
(Sn-3.5Ag)-Al	Cu_6Sn_5, Cu_3Sn IMC layer and Cu-Al and Ag_3Al particles	Ni_3Sn_4,NiPSn, Ni_3P IMC layer and Al_3Ni_2 and Ag_3Al particles

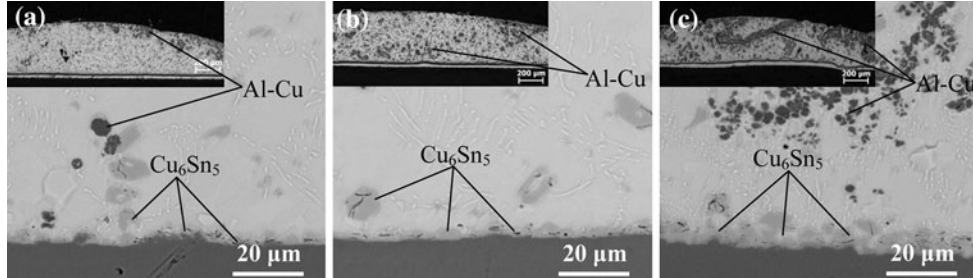

Fig. 11. SEM images showing interfacial reactions of: (a) (Sn-3.5Ag)-0.5Al/Cu, (b) (Sn-3.5Ag)-1Al/Cu, and (c) (Sn-3.5Ag)-2Al/Cu systems, after reflow at 260°C for 60 s.

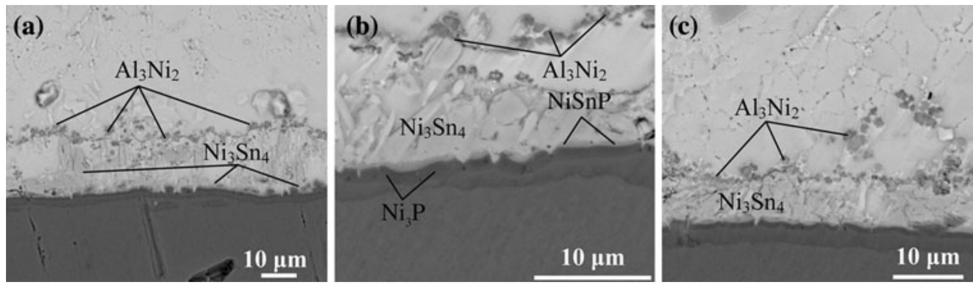

Fig. 12. SEM images showing interfacial reactions of: (a) (Sn-3.5Ag)-0.5Al/Ni(P), (b) (Sn-3.5Ag) 1Al/Ni(P), and (c) (Sn-3.5Ag)-2Al/Ni(P) systems, after reflow at 260°C for 60 s.

Table VI. Observed differences between the Sn-Ag-Zn and Sn-Ag-Al systems on Cu and Ni(P) substrates in terms of IMC suppression and spalling

	Alloying Elements	
Substrate	Zn	Al
Cu	Suppression of Cu_6Sn_5 and Cu_3Sn interfacial IMC	Al-Cu particles form in solder matrix, instead of forming interfacial Al-Cu IMC layer as occurs in solder bath studies[11]
	Massive spalling[16] of Cu-Zn IMC layer, forming a Cu-Zn barrier layer when Zn ≥1 wt.%	No suppression of interfacial IMCs (Cu_6Sn_5 or Cu_3Sn)
	Spalling Cu_6Sn_5 from Cu[5,23–25] substrate when Zn >1 wt.%, during aging at 150°C	
Ni(P)	Spalling Ni_3Sn_4 from Ni(P) substrate[25] during aging at 150°C	Al-Ni particles initially form at interface, but continuous layer is not formed, allowing Ni_3Sn_4 growth. Note that Al-Ni particles are not formed in solder matrix in contrast to Cu due to slower dissolution rate of Ni
	Suppression of Ni_3Sn_4 IMC due to formation of $(Ni_{1-x}, Zn_x)_3Sn_4$ interfacial IMC	

the Al_3Ni_2 IMC particles are located in a discontinuous layer ~5 μm from the Ni(P) substrate, rather than at the substrate interface. The location of the layer suggests that the IMC originally formed at the solder/substrate interface before being replaced by Ni_3Sn_4. The discrepancy with Ref. 11, where the Ni-Al IMC barrier layer remained at the interface, is attributed to the limited volume of solder used in this study. As the concentration of Al in the solder is increased, the concentration of Al-Cu and Al-Ni IMC particles in the solder matrix increases, without affecting the growth rate of the Cu-Sn and Ni-Sn IMC layers.

ACKNOWLEDGEMENTS

This research was funded by the Engineering and Physical Sciences Research Council (Grant No. EP/G054339/1) in collaboration with Henkel Technologies, Dynex, and Schlumberger. The authors thank Dr. Anthony Brain for help with microscopy.

REFERENCES

1. J. Glazer, *Int. Mater. Rev.* 40, 65 (1995).
2. M. Abtew and G. Selvaduray, *Mater. Sci. Eng. R* 27, 95 (2000).
3. K. Zeng and K.N. Tu, *Mater. Sci. Eng. R* 38, 55 (2002).
4. K.N. Tu, A.M. Gusak, and M. Li, *Appl. Phys. Rev.* 93, 1335 (2003).
5. K.N. Tu, *Solder Joint Technology: Materials, Properties, and Reliability.* Springer, New York, USA (2007).
6. H.F. Zou, H.J. Yang, and Z.F. Zhang, *Acta Mater.* 56, 2649 (2008).
7. J.F. Li, S.H. Mannan, M.P. Clode, D.C. Whalley, and D.A. Hutt, *Acta Mater.* 54, 2907 (2006).
8. J.F. Li, S.H. Mannan, M.P. Clode, D.C. Whalley, and D.A. Hutt, *Acta Mater.* 55, 737 (2007).
9. F. Wang, X. Ma, and Y. Qian, *Scripta Mater.* 53, 699 (2005).
10. Y.K. Jee, Y.H. Ko, and J. Yu, *J. Mater. Res.* 22, 1879 (2007).
11. Y.K. Jee, Y.H. Xia, J. Yu, H.W. Kang, and T.Y. Lee, *IEEE 58th Electronic Components and Technology Conference* (Florida, May 2008), pp. 491–494.
12. Y.H. Xia, Y.K. Jee, J. Yu, and T.Y. Lee, *J. Mater. Res.* 37, 1858 (2008).
13. S.K. Kang, D.Y. Shih, D. Leonard, D.W. Henderson, T. Gosselin, and S. Cho, *JOM* 56, 34 (2004).
14. M. Lu, D.Y. Shih, S.K. Kang, C. Goldsmith, and P. Flaitzb, *J. Appl. Phys.* 106, 053509 (2009).
15. H.R. Kotadia, O. Mokhtari, M. Bottrill, M.P. Clode, M.A. Green, and S.H. Mannan, *2010 International Symposium on Advanced Packaging Materials: Microtech Conference* (Cambridge, March 2010), pp. 17–21.
16. C.M.L. Wua, D.Q. Yua, C.M.T. Lawa, and L. Wangb, *Mater. Sci. Eng. R* 44, 1 (2004).
17. A. Fawzy, *Mater. Character.* 58, 323 (2007).
18. M. McCormack and S. Jin, *JOM* 45, 36 (1993).
19. C.Y. Yu, K.J. Wang, and J.G. Duh, *J. Electron. Mater.* 39, 230 (2010).
20. http://gow.epsrc.ac.uk/ViewGrant.aspx?GrantRef=EP/G054339/1.
21. S.C. Yang, C.E. Ho, C.W. Chang, and C.R. Kao, *J. Appl. Phys.* 101, 084911 (2007).
22. C. Chou and S. Chen, *Acta Mater.* 54, 2393 (2006).
23. J.M. Koo, B.Q. Vu, Y.N. Kim, J.B. Lee, J.W. Kim, D.U. Kim, J.H. Moon, and S.B. Jung, *J. Electron. Mater.* 37, 118 (2007).
24. X. Wang, Y.C. Liu, and Z.M. Gao, J. Mater. Sci.: Mater Electron. (2010). doi:10.1007/s10854-010-0075-1.
25. J.W. Ronnie Teo and Y.F. Sun, *Acta Mater.* 56, 242 (2008).
26. D. Yao and J.K. Shang, *IEEE Trans. CPMT B* 19, 154 (1996).
27. M.G. Cho, S.K. Kang, D.Y. Shih, and H.M. Lee, *J. Electron. Mater.* 36, 1501 (2007).
28. V.I. Dybkov, *Growth Kinetics of Chemical Compound Layers* (Cambridge: Cambridge International Science, 1998).
29. R. Ashayer, A. Cobley, O. Mokhtari, S.H. Mannan, S. Sajjadi, and T. Mason, *ESTC, Greenwich,* Vol. 1–2 (2008), pp. 929–933, ISBN 978-1-4244-2814-4.
30. F. Wang, F. Gao, X. Ma, and Y. Qian, *J. Electron. Mater.* 35, 1818 (2006).
31. W.F. Feng, C.Q. Wang, and M. Morinaga, *J. Electron. Mater.* 31, 185 (2002).